

Structure and photocatalytic properties of the composite coating fabricated by detonation sprayed Ti powders

V.V. Sirota^{a,*}, V.S. Vashchilin^a, Y.N. Ogurtsova^a, E.N. Gubareva^a, D.S. Podgornyi^a, M.G. Kovaleva^b

^a Belgorod State Technological University named after V.G. Shoukhov, 46 Kostyukova Str., Belgorod, 308012, Russia

^b Belgorod State National Research University, 85 Pobedy Str., Belgorod, 308015, Russia

ARTICLE INFO

Handling Editor: Dr P. Vincenzini

Keywords:

Composite coatings based on titanium oxides
Detonation spray coating process
Microstructure
Photocatalytic activity

ABSTRACT

In the present study, composite coatings based on titanium oxides were successfully prepared using detonation spray coating process on two types of substrates: hot-rolled carbon steel and fine-grained hyperpressed concrete. The microstructure, phase composition and photocatalytic activity of these coatings were investigated. The structure of the coatings presents many lamellae piled up one upon another, and is composed of rutile, anatase, titanium oxide, and titanium. Coatings were studied for the photocatalytic degradation of organic pollutants such as methylene blue (MB) and rhodamine B (RhB) under UV light. The photocatalytic activity of the composite coatings based on titanium oxides also was evaluated by changing the contact angle. The results showed that composite coatings based on titanium oxides have a high photocatalytic activity on surfaces of the hot-rolled carbon steel and fine-grained hyperpressed concrete. Taking into account the results presented in this work, it is expected that the produced coatings can later be used as effective photocatalysts and can become the basis for detonation deposition of protective self-cleaning composite coatings based on TiO₂.

1. Introduction

The problem of biocorrosion is one of the main factors that reduce the service life of equipment, building products and structures, such as marine machinery and equipment, treatment facilities, port infrastructure, etc. [1]. Global urbanization causes pollution of the human environment with organic waste and pathogenic microorganisms [2–4].

Protective coatings can be considered as a possible solution, which can significantly extend the service life and delay the process of restoration or complete replacement of individual elements of devices, materials or entire structures as much as possible. An example of such coatings is photocatalytic coatings. This is a special class of materials, the nanosized particles of the photocatalyst included in such a coating, under the action of radiation, ultraviolet or visible spectrum, are able to decompose the molecules of many pollutants due to the formation of OH and O₂^{•-} decomposing organic matter into CO₂ and H₂O [5,6], killing algae, fungi and bacteria during this process. This ability allows such coatings to be effectively used as an important element of environmental maintenance and cleaning systems.

Due to the photocatalytic properties, the presented coatings are able

to protect materials from the progressive reproduction of microorganisms and have the ability to self-clean from all kinds of pollutants deposited on the surface, which is also a very relevant criterion at present.

Typical photocatalysts include: ZnO, TiO₂, CuO, MgO, Ag₃PO₄, Cu₂O, NiCo₂O₄, α-NiMoO₄, CoFe₂O₄, Mg₂TiO₄, WO₃, Ag₂MoO₄, and Bi₂MO₆ [7].

One of the most accessible and efficient photocatalysts is TiO₂ in the anatase polymorph. Other polymorphic modifications, rutile and brookite, also show photocatalytic activity, but much lower than that of anatase [8,9].

The most common application of TiO₂ as photocatalyst is the deposition of coatings on the surface of objects, which should have bactericidal and cleaning properties [10]. For the deposition of titanium oxide, the commonly used the sol-gel method [11–15], the combustion method [16], the deposition of TiO₂ in the composition of polymers, adhesives and paints [17–21], the chemical vapor deposition (CVD) method [22–26], physical vapor deposition (PVD) [27–30], and the thermal spraying methods [31–38]. However, every coating technique has its advantages and limitations to some extent. Sol-gel deriving processes

* Corresponding author.

E-mail address: v-sirota@list.ru (V.V. Sirota).

<https://doi.org/10.1016/j.ceramint.2023.10.152>

Received 30 May 2023; Received in revised form 3 October 2023; Accepted 16 October 2023

Available online 21 October 2023

0272-8842/© 2023 Elsevier Ltd and Techna Group S.r.l. All rights reserved.

such as dip- or spray-coating are the most widely employed. Both these procedures present some disadvantages in a view of a large scale application: the complexity, low reproducibility of processes, and insufficient coating thickness [39]. PVD and CVD methods require large and complicated equipment and vacuum conditions, and they have high fabrication costs [40].

The thermal spraying process has many advantages, including its low cost, thicker coatings that can be formed quickly, a wide selection of materials, and a process that is simpler than other coating processes [41, 42]. Therefore, thermal spraying, especially atmospheric plasma spraying (APS) [41] and high velocity oxy-fuel spraying (HVOF) [43], are the preferred option and are widely used in the production of TiO₂ coatings that improve the biocompatibility of metal substrates [31].

In the works [31,44–47] TiO₂ coatings were deposited by suspension plasma spraying, low-pressure cold gas spraying and high velocity oxy-fuel spraying. The coatings were a dense deposit with characteristic packing, involving regions of partially melted or unmelted particles alternating with zones consisting of well-melted particles (the crystalline phase is randomly mixed with the amorphous phase).

The values of the kinetic constant for these coatings were, in every case, much higher than that for a commercial sol-gel coating. The correlation coefficients were higher than 0.988, indicating a reasonably good fit of the kinetic model to the experimental data. A similar fit was found by Toma et al. [48] with suspension plasma sprayed titanium coatings, though the rate constants were quite different owing to the different test conditions and chemical reagent used.

Thermal spraying often has problems with the oxidation of raw materials and the presence of undesirable oxide phases, which reduce the quality of the substrate/coating interface and affect the properties of coatings [49].

There are works on the formation of coatings based on titanium dioxide also by the method of detonation spraying of powders. The features of this method are the high temperature of the carrier gas, the high speed of the sprayed powder and the temperature at the moment of impact of the powder on the substrate. Recent developments in the detonation spraying make it attractive for producing dense coatings of good adhesion [49–55].

The present study was undertaken to prepare photocatalytic composite coatings based on titanium oxides using a robotic complex for detonation spraying of coatings (IntelMashin LLC, Moscow, Russia) equipped with a multi-chamber detonation accelerator (MCDS) [53–64]. The microstructure, phase composition and photocatalytic activity of these coatings were investigated. Hot-rolled carbon steel and fine-grained hyperpressed concrete were used as substrates.

2. Materials and methods

2.1. Coating deposition

As a material for spraying, we used powder of titanium (grade PTS-1) produced by JSC Polema (Russia) (d(0.1): 11.29 μm, d(0.5): 48.63 μm, d(0.9): 91.31 μm). A fraction of 40–60 μm was preliminarily selected by the sieve method. The morphology and composition of the titanium powder, according to scanning electron microscopy (SEM, TESCAN MIRA 3 LMU, Brno-Kohoutovice, Czech Republic), is shown in Fig. 1, a. The particle size distribution was measured by the laser scattering method using a particle size analyzer (Analysette 22 NanoTec Plus, Fritsch GmbH, Idar-Oberstein, Germany) (Fig. 1, b). The phase analysis shows that the main phase in the titanium powder is Ti with a hexagonal lattice structure ($a = b = 2.94 \text{ \AA}$, $c = 4.68 \text{ \AA}$) (Fig. 1, c). The powder was

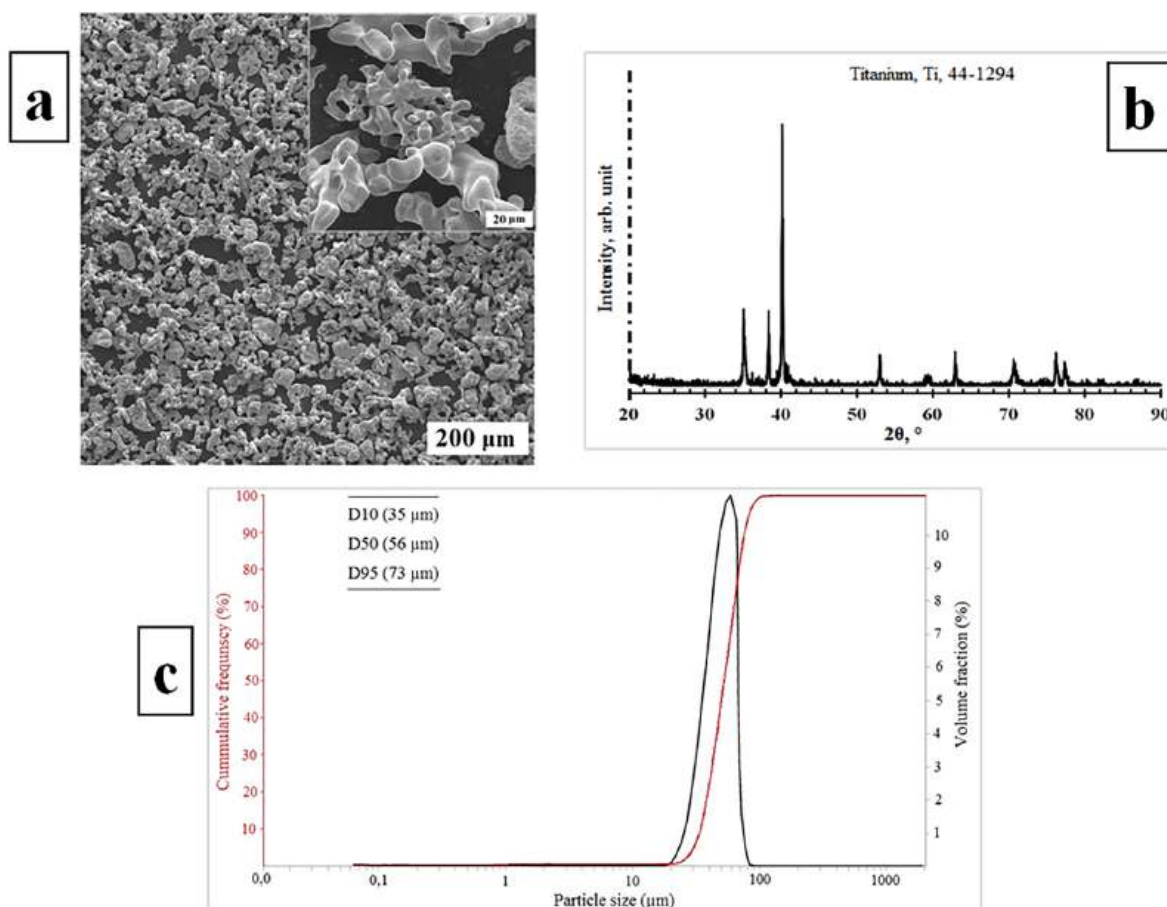


Fig. 1. The titanium powder: SEM micrograph (a), XRD pattern (b), and particle size distribution (c).

dried in an electric oven at 200 ± 5 °C for 60 min to reduce agglomeration and eliminate the possibility of sticking during the detonation spray coating process.

Formation of the composite coatings based on titanium oxides was carried out using a robotic complex for detonation spraying of coatings (IntelMashin LLC, Moscow, Russia) equipped with a multi-chamber detonation accelerator (MCDS) (Fig. 2) [53–64].

In our previous work [65] the efficiency of the MCDS was compared to that of the best samples of a wide variety of units for thermal spraying of coatings, which provide a high velocity of spraying powder and minimal porosity of the resulting coating. The MCDS is advantageous over other units in that it requires a much lower consumption of fuel gases and electric power at the same quality of coatings. Pressure in the gas lines is not in excess of 0.4 MPa. Design peculiarities of the unit allow the spraying process to be performed without overheating of device's parts and without damaging them. The difference between MCDS and high-speed gas-thermal methods is that it sums up the energies of combustion products of fuel gas mixtures from several specially profiled detonation chambers. The rate and temperature of the combustion products depend only on the parameters of filling of each chamber with the fuel gas mixture. The accumulation of detonation energy from the two chambers in the cylindrical nozzle provides high-speed jet forming combustion products that effectively heat and accelerate the powder material. With MCDS technology, the energy of the fuel gas mixture was transformed into a high-velocity jet with a low thermal power, which allows the formation of a high-quality layer with no overheating of a workpiece. The high combustion initiation frequency (20–30 Hz) and MCDS provide the possibility of implementing the quasi-continuous coating technology. This allows employing standard devices for feeding gases and powder under a low pressure. The MCDS was equipped with a standard powder feeder (by Metco).

MCDS device can be used horizontally, vertically as well as at an angle to the sprayed surface for deposition of the coating on the inner surface of the product. The use of MCDS makes it possible to form high-speed pulsed jets of heated ceramic powders (2100 ± 100 m/s), which provide the ability to create high contact loads upon the impact of discrete particles on the substrate surface, making it possible to deform ductile and destroy fragile substrate materials [53,60,61,66].

Low thermal power of the combustion products permits formation of coatings from a small distance (20–80 mm), this providing a substantial increase in spraying efficiency and decrease in oxidation and losses of a

spraying material. Coatings can be deposited on small-size pieces with thin walls (0.3–1.0 mm), this widening the application field for the technology. The technology is of the pulsed type. The combustion products contact the walls of the combustion chambers for $1\text{--}2 \cdot 10^{-3}$ s, this decreasing the MCDS thermal intensity and cooling costs. In addition, the use of initial low-pressure gases (0.1–0.3 MPa) allows the control panels to be fitted with simple standard devices, thus reducing the price of the equipment and, what is most important, improving the operational safety. The use of the low-pressure process gases considerably increases the efficiency of utilization of gas bottle systems.

As substrates, 40 x 40 mm samples were made from hot-rolled carbon steel (Fe–0.25C–0.90Mn–0.04P–0.05S–0.20Cu, all in wt pct) and fine-grained hyperpressed concrete. Before coating, the target surface was degreased and sandblasted. The surface roughness (Ra) of specimen after sandblasted was 3.50 ± 0.15 μm. The parameters of the composite coatings based on titanium oxides spray are listed in Table 1. The gas flow rate was determined using float flowmeters.

2.2. Sample characterization

The study of the structure and distribution of elements in the coating material was carried out by scanning electron microscopy (SEM, TESCAN MIRA 3 LMU, Brno-Kohoutovice, Czech Republic). The specimens were transversally cut, mechanically polished and prepared by standard metallographic methods-sectioning, mounting and polishing - for sample preparation. The sample was prepared by grinding with SiC sandpapers with various specifications (200, 500, 800 and 1000#), followed by polishing with 1-μm diamond slurry according to the procedure recommended by Struers company for ceramic coatings. The specimens were cleaned with distilled water and dried at 100 °C for 3 h [60].

The analysis of the distribution of the elements on the surface and in the volume of the coating was studied by energy-dispersive X-ray spectroscopy (EDX).

Porosity of the coating was determined by metallographic method with elements of the qualitative and quantitative analyses of the geometry of the pores using an optical inverted Olympus GX51 microscope (Olympus Corporation, Tokyo, Japan) [67]. The images were registered in an optical microscope, in bright field, magnified $500 \times$. The image acquisition of the structure of the studied layer was done using "SIAMS Photolab" programme. At least ten arbitrarily selected typical micrographs were analyzed for each experimental point.

Phase composition of the powder and coatings was determined by the X-ray phase analysis method (diffractometer ARL 9900 WS). An ARL 9900 WS X-ray powder diffractometer using Co-K α monochromatic radiation (wavelength $\lambda = 1.788996$ Å) operating at 30 kV and 30 mA was employed to determine the X-ray diffraction patterns. XRD spectrum for phase analysis was determined by shooting the scheme θ - θ scan focusing by Brega–Brentano in the angular range of 8–80 2θ . Investigations were carried out in $\theta/2\theta$ step scan mode at a step of 0.02 in 2θ range at a rate of 0.5/min. Crystalline phases were identified by the ICDDPDF-2 (2008) powder diffraction database. Quantification of weight fractions of individual crystalline phases was done by Rietveld refinement analysis in SiroQuant software [68,69].

The surface roughness (Ra) of substrate was measured by a Taylor–Hobson Surtronic 25 Profilometer (see Table 1). Tests were performed at 25 °C with a relative humidity of approximately 50 %.

2.3. Evaluation of photocatalytic activity

2.3.1. Determination of photocatalytic activity of sample surface by degradation of methylene blue

Methylene blue (MB) as a common organic dye is frequently used as the target degradation pollutant in the photocatalytic activity evaluation of TiO₂ [70].

Photocatalytic activity of the samples was evaluated by measuring the degradation rate of MB solution at room temperature in accordance



Fig. 2. A new robotic complex for detonation spraying of coatings (IntelMashin LLC, Russia) equipped with a multi-chamber detonation accelerator (MCDS).

Table 1

Parameters of composite coatings based on titanium oxides deposition by a robotic complex for detonation spraying of coatings.

Barrel length, mm	Barrel diameter, mm	Deposition distance, mm	Powder Feed Rate, g/h	Flow rate of fuel mixture components, m ³ /h		
				Air	Oxygen	Propane
300	16	60	800	1.3*/1.54**	2.44*/3.04**	0.56*/0.67**

*Cylindrical form combustion chamber. **Combustion chamber in the form of a disk.

with the recommendations of ISO 10678:2010 (E) [71] and using a double-beam spectrophotometer “PE-6100” (Promecolab, Russia) with quartz cuvettes with an optical thickness of 10 mm at a wavelength of 664.5 nm.

Samples after ultrasonic cleaning were spread uniformly on the bottom of cuvettes. To obtain the same initial conditions for all the samples, MB solution (50 ml, 3 μmol/L) was preadsorbed onto the samples before evaluating photocatalytic activity. The cuvettes were closed with special plastic caps to prevent evaporation of the solution. The cell containing the samples and MB solution were kept in the dark for 24 h to allow adsorption.

The photocatalytic activity of each sample was evaluated under ultraviolet (UV) light (UV lamp TL-D 36W/08 BLB) with an intensity of 1 mW/cm² for 5 h with stirring of the solution and taking the results on a spectrophotometer with an interval of 1 h.

The photocatalytic activity score (ED_{MB},%) was calculated using equation (1):

$$ED_{MB} = \frac{(C_0 - C_5)}{C_0} \times 100\%, \quad (1)$$

where: C₀, C₅ are the concentrations of methylene blue solutions before and after irradiation for 5 h, respectively.

For each sample five measurements were performed and the average value was considered.

2.3.2. Determination of the photocatalytic activity of hydraulic binders Radamina test method

The photocatalytic activity of sample surface was determined by the method of decolorization of an organic rhodamine B dye (RhB) in accordance with the UNI 11259 standard [72]. This standard describes a method to determine the photocatalytic activity of hydraulic binders by a colorimetric test method.

The RhB is used as a surrogate to simulate particulate pollutants because its structure resembles some airborne particulate compounds. The RhB was extensively used in studies [73,74] to demonstrate the self cleaning efficiency.

The removal efficiencies of particulate pollutants in this study were evaluated based on the degradation of RhB under UV irradiation. The photocatalytic efficiency was evaluated by monitoring the discoloration of rhodamine B applied to the surface of the materials which were then exposed to artificial sun light.

Rhodamine B was dissolved in de-ionised water to achieve a concentration of 4·10⁻⁴ mol/L. One milliliter of this RhB solution was applied on the surface of samples. The samples were allowed to dry for 30 min at a temperature of 20 ± 1 °C at a relative air humidity of 60 ± 10 % before being exposed to UV irradiation (UV lamp with an illumination of ultraviolet radiation 2.50 ± 0.25 mW/m²). Due to the photocatalytic effect of TiO₂, color intensity on the specimen surface will decrease with an increased exposure to UV irradiation.

The degree of degradation of the organic pollutant from the surface of the composite material was studied by the colorimetric method using the a* coordinate of the Commission International d’Eclairage (CIE) LAB system. L* - describes the brightness from black to white, a* - reflects the values between red and green, b* - between blue and yellow [72–74].

The evaluation of the degree of decomposition of rhodamine B is based on a comparison of the color parameter a* before and after exposure to ultraviolet radiation on the surface of the test sample for 4

and 26 h. The removal efficiency of the dye was calculated by equations (2) and (3):

$$R_4(\%) = \frac{a_0^* - a_4^*}{a_0^*} \times 100\% \quad (2)$$

$$R_{26}(\%) = \frac{a_0^* - a_{26}^*}{a_0^*} \times 100\% \quad (3)$$

where R₄ and R₂₆ are the degree of discoloration of the dye after 4 h and 26 h of exposure to UV irradiation, respectively; a*(0h), a*(4h), a*(26h) are the color parameter of the dye surface before irradiation (0h) and after irradiation with UV light for 4 h and 26 h, respectively. Under the conditions R₄>20 % and R₂₆>50 %, the material under study is photocatalytic [72,75].

For each sample five measurements were performed and the average value was considered.

2.3.3. Determination of the photocatalytic activity by changing the contact angle

The photocatalytic activity of the composite coatings based on titanium oxides was evaluated by changing the contact angle (wetting angle) under the influence of ultraviolet radiation in accordance with ISO 27448:2009 (Fine ceramics (advanced ceramics, advanced technical ceramics) - Test method for self-cleaning performance of semi-conducting photocatalytic materials - Measurement of water contact angle”) [75]. This test method is to evaluate the self-cleaning performance of a photocatalytic material by obtaining the final contact angle (wetting angle) of a test piece on which organic substances are applied. The organic substance is first applied to a test piece (pretreatment), which is then irradiated by ultraviolet radiation (UV-A, illumination (2.0 ± 0.1) mW/cm²) at a constant intensity. The effectiveness of the self-cleaning ability of a material is evaluated by the time to reach the final contact angle after the start of irradiation. This test simultaneously evaluates the decomposition of the organic substance (oleic acid, which acts as an organic “pollutant”) and change of water affiliation.

The effectiveness of the self-cleaning ability of a material is evaluated by the time to reach the final contact angle after the start of irradiation, which according to ISO 27448:2009 should be no more than 80 h for the material to be considered photocatalytically active self-cleaning.

For each sample five measurements were performed and the average value was considered.

3. Results and discussions

3.1. Structure and phase composition of the composite coatings based on titanium oxides

Fig. 1a and 1,b show the cross-sectional SEM images of composite coatings based on titanium oxides on substrates of hot-rolled carbon steel and fine-grained hyperpressed concrete respectively. The light and dark areas of these coatings were confirmed to be Ti and Ti_xO_y by energy dispersive X-ray analysis (SEM-EDX), respectively. The cross-section of the coated sample (Fig. 3) reveals a defect-free structure showing a sufficiently dense structure. The coatings have thicknesses about 150–200 μm. The thickness of the composite coatings based on titanium oxides on substrate of hot-rolled carbon steel was 100–150 μm. The thickness of the composite coatings based on titanium oxides on fine-

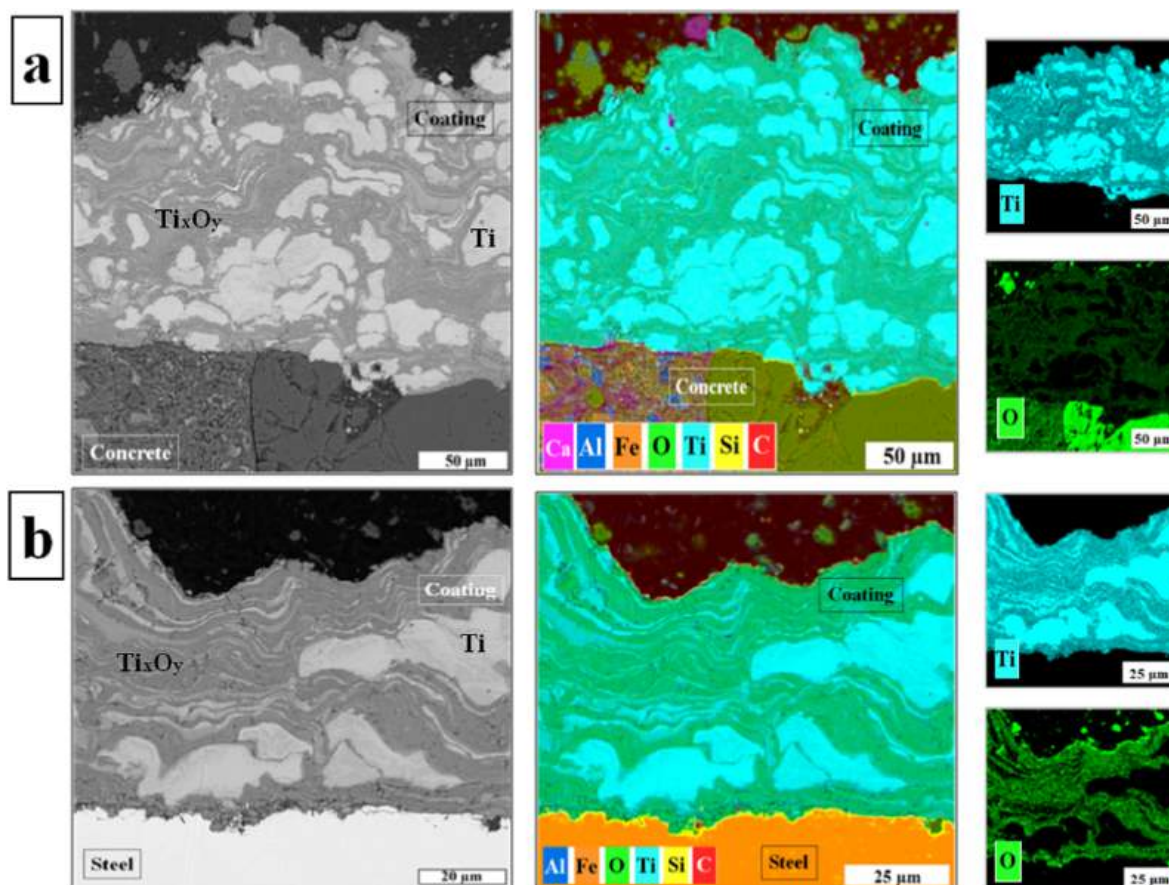


Fig. 3. SEM micrographs (back-scattered electron mode) and SEM EDX element distribution maps of the cross-section of the composite coatings based on titanium oxides on the fine-grained hyperpressed concrete (a) and hot-rolled carbon steel (b).

grained hyperpressed concrete was 150–200 μm . The difference in coating thickness is associated with an increase in the coating time to fill defects and pores on the concrete surface. Most of the powder particles melted (fully melted area). It was found that the shape of the fully melted area had a lamellar-like structure (typical for thermally sprayed coatings [53,56,76,77]) with splats built from completely resolidified TiO_2 . The reason is that the high velocity of the particles impacting under relatively cold conditions onto the substrate, results in the disintegration of the powders. The coatings exhibit some particles disturbing the general arrangement of lamellas aligned perpendicularly to the spraying direction. Such particles are not flattened well at impact because of the low impact velocity, but they retain the original size and shape of the feedstock.

At the beginning of the coating build-up, particles impact directly onto the substrate. The spraying torch moves over the substrate and the first layer is usually composed of 5–15 lamellae. The first seconds of the deposition process ensure the formation of well separated areas of deposits in the surface layer. The process of fixing of heated particles takes place in the recesses. In the impact zone, the material of the powder and substrate are strongly plasticized and deformed, which provides all the necessary conditions for the coating formation. Upon impact, part of the kinetic energy of the powder particle is spent on its deformation and the substrate deformation.

In the subsequent seconds the torch returns to the same spot and a high-speed powder jet impact on the surface ensures the formation of a continuous layer of coating that covers the entire surface. The surface of the layer is subjected to cooling. The molten particles deform, become lamellated and solidify into columnar or fine-grained equiaxial crystals. During spraying of the next layer of coating, the torch also heats up the previously deposited material by convection.

Additional heat fluxes result from solidification of the particles and their cooling down to the temperature of equilibrium. The final coating's thickness is reached in a few passes of the torch over the substrate [59].

The porosity of the coating was about 1.0 % with a standard deviation of 0.22 %. Fig. 1 shows good adhesion between the coating and the substrate, with no penetrating cracks or voids across the coating.

The EDX element distribution maps in the volume and on the surface of composite coatings are shown in Figs. 3 and 4. They illustrate uniformly distributed Ti and O in the volume and on the surface of composite coating based on titanium oxides.

For a fast and highly non-equilibrium process of detonation spraying, it is very difficult to predict the extent of chemical reactions that occur between the powders and the gaseous phase [78]. As the particles leave the barrel, they enter the surrounding atmosphere, and interact with air [79]. The oxidation reaction of titanium proceeds at the highest rate compared to its interaction with other gases [80]. The formation of oxide phases in the coating is due to the oxygen content in the gas mixture and its interaction with the titanium powder during the coating process. Titanium exists in different oxidation states: Ti^{2+} , Ti^{3+} , and Ti^{4+} . The corresponding oxides are TiO , Ti_2O_3 , Ti_3O_5 , TiO_2 .

The results of X-ray diffraction analysis of the composite coatings based on titanium oxides are given in Fig. 5 and Table 2. The distinguished interplanar spacing calculated from reflections makes it possible to identify the following phases in the coatings: anatase (PDF No. 21–1272) and rutile (PDF No. 21–1276) with tetragonal lattice structure, Ti_2O_3 with rhombohedral lattice structure (PDF No. 71–1056), TiO with a monoclinic lattice structure (PDF No. 23–1078), and Ti with a hexagonal lattice structure (PDF No. 44–1294). This means that in this study, using the coating parameters, oxidizing conditions were created that convert almost all titanium into its oxides, including stable ones

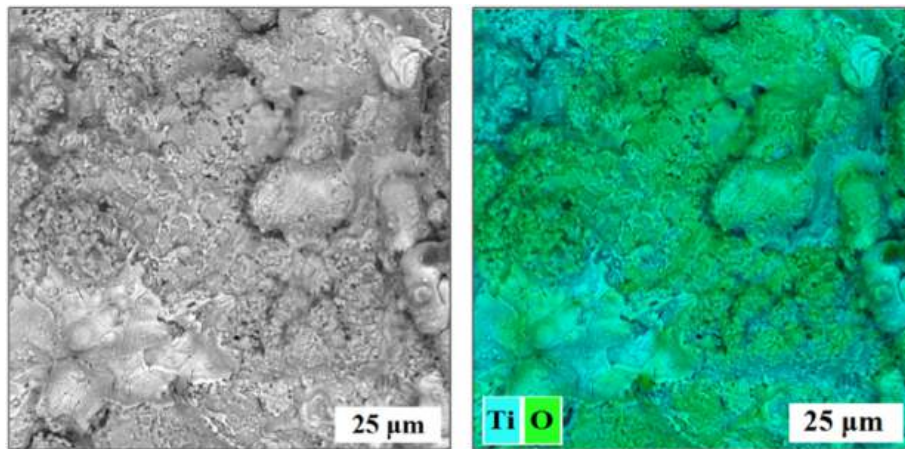


Fig. 4. SEM micrograph (back-scattered electron mode) (a) and SEM EDX element distribution map of the surface of the composite coating based on titanium oxides (b).

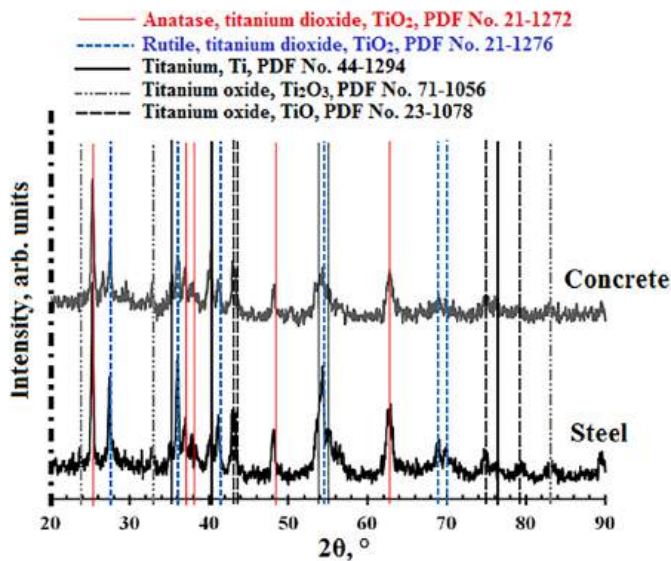


Fig. 5. Results of X-ray diffraction analysis of the composite coating based on titanium oxides.

Table 2

Phase composition of the composite coatings based on titanium oxides.

Phases	Phase quantity, %	
	Steel substrate	Concrete substrate
rutile (TiO ₂)	44.5	36.0
anatase (TiO ₂)	22.3	24.0
titanium oxide (TiO)	20.0	20.0
titanium oxide (Ti ₂ O ₃)	3.3	7.1
titanium (Ti)	9.9	12.9

[55,81]. It can be seen that the coating was composed of rutile (TiO₂), anatase (TiO₂), titanium oxide (TiO), titanium oxide (Ti₂O₃), and titanium (Ti) (Table 2).

A key issue throughout all latest research has been the preservation of the largest possible quantity of anatase phase in the coating, because of the superior photocatalytic performance of anatase compared to that of rutile [44]. However, controversy persists with regard to the factors that control TiO₂ phase (anatase versus rutile) distribution in the final layers. A mixture of anatase and rutile is always encountered, regardless of the nature and composition of the feedstock, while anatase

and rutile contents can vary widely [82,83].

The lack of linear correlation between anatase content and photocatalytic activity was already reported by Toma et al. [84]. Kozerski et al. [85] recently confirmed this lack of correlation and demonstrated the photocatalytic activity of suspension plasma sprayed titania coatings that consisted mainly of rutile.

As a rule, the substrate itself should not interfere with the photocatalytic material deposited on its surface, nor should it affect its photocatalytic activity, which thus makes it possible to obtain more objective results regarding the pure photocatalytic activity of the material itself under various experimental conditions [86]. It can be seen from Table 2 that at identical coating deposition parameters the quantity of anatase phase in the coating on concrete substrate is insignificantly greater than in the coating on steel substrate. This result is due to the difference in the thermal conductivity of steel and concrete. A steel target heats up strongly during sputtering, while a concrete target heats up much less.

3.2. Photocatalytic activity by MB degradation

The photocatalytic activity was investigated based on the degradation of MB in an aqueous solution under ultraviolet (UV) light. MB has a maximum absorption of approximately 664 nm.

The analysis of the entire range of the time-dependent UV–V absorption spectra shows that the intensity of MB absorption band decreases gradually, without revealing any new band in the spectra confirming lack of reaction by-product, and therefore, as the degradation is stable (Fig. 6). Based on the change of the intensity of the peak centered at 663 nm, the UV degradation rate of the dye was plotted as C/C₀ versus time (where C₀ and C are the initial concentration and the concentration of dye after different time of photo irradiation, respectively).

Clear differences were found in the solution concentrations at each irradiation time. The concentration of the blank (marked with reference solution) hardly decreased, which hints the MB solution did not degrade. In the composite coatings based on titanium oxides sample-containing reactor, there is a visible decrease in the peak intensity of the azo bond (664 nm) assisted by degraded of MB solution under the action of composite coatings based on titanium oxides and UV irradiation. It indicates that the composite coatings based on titanium oxides showed photocatalytic activity toward MB solution.

As can be seen on the plot, composite coatings based on titanium oxides strongly adsorb MB under dark (Fig. 6, a). This could be attributed to the high specific surface area and small particle size [87].

Similar results were obtained for all coatings sprayed on to both steel and concrete substrates. In addition, MB initial adsorption at the end of

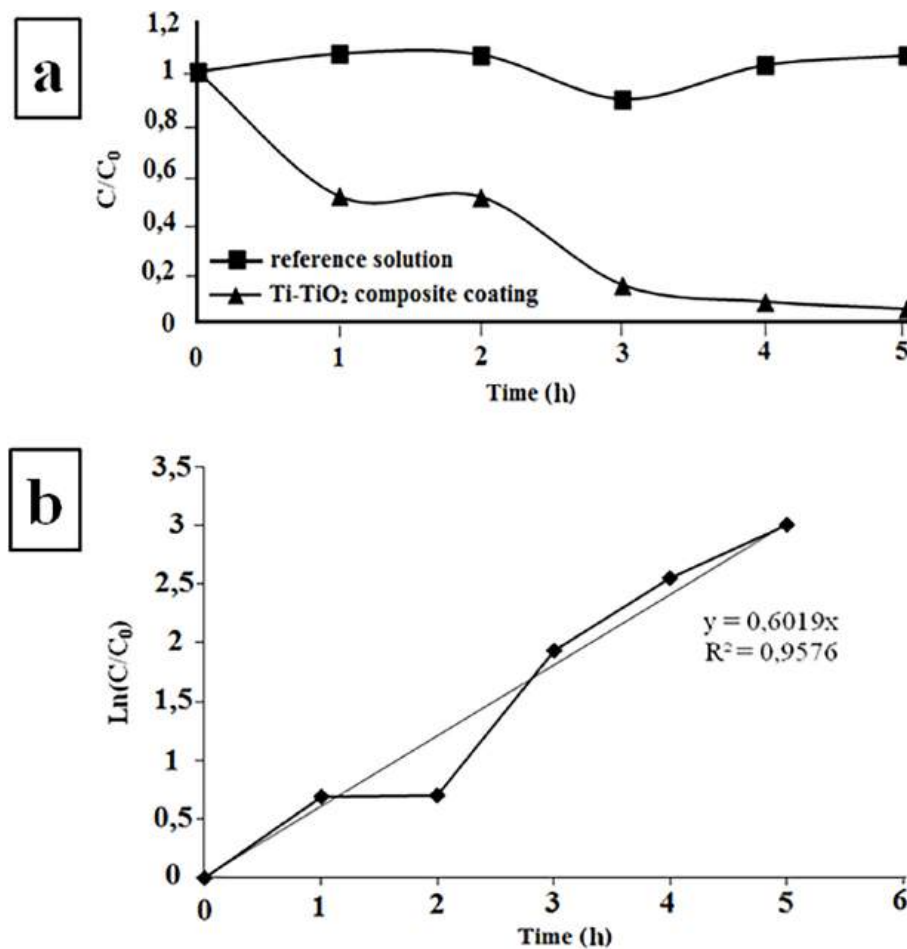


Fig. 6. The decolorization ratio of MB (a) and the apparent first-order linear transforms in the presence of the sample with composite coatings based on titanium oxides (b).

soaking time in the dark was quite small in every case, confirming the low porosity found in the coatings.

Not only the degradation efficiency but also MB decomposition kinetics was determined (Fig. 6, b). The shape of curve is in good agreement with the results of other works [44,88–90] and suggested pseudo-first order kinetic rate plot which can be described by the widely accepted in heterogeneous photocatalysis Langmuir-Hinshelwood (LH) kinetic model (4):

$$\ln \frac{c}{c_0} = -kt, \quad (4)$$

where: k is the rate constant of the photocatalytic reaction in h^{-1} ; t is the irradiation time in h; c_0 and c are the concentration of the dye after darkness adsorption and the concentration of the dye measured at the time point t , respectively.

Fig. 6,b shows the pseudo-first order reaction of the photocatalytic degradation kinetics of methylene blue on composite coatings based on titanium oxides.

The degradation rate constants (k value) were calculated to be 0.602 h^{-1} (Fig. 6,b) for samples with composite coatings based on titanium oxides, which is much higher than k for TiO_2 coatings obtained by other methods [74,87–91]. For example, in the works [44,88] the constant of the rate of photocatalytic reaction (k) was $0.105\text{--}0.155 \text{ h}^{-1}$ for TiO_2 coatings are obtained by the method of suspension plasma spraying and by the sol-gel method on steel substrate.

The correlation coefficient for composite coatings based on titanium oxides was higher than 0.9577, indicating a reasonably good fit of the kinetic model to the experimental data. The photocatalytic activity of

EDMB (%) calculated by equation (1) was 95 %.

3.3. Photocatalytic activity by decolorization of rhodamine-B

The photocatalytic activity was assessed as discoloration of rhodamine B (RhB) aqueous solution on substrates (hot-rolled carbon steel, fine-grained concrete) and composite coatings based on titanium oxides. Tests prove an increase in the photocatalytic performances of hot-rolled carbon steel and fine-grained concrete substrates by deposition of composite coating based on titanium oxides (Table 3 and Fig. 7).

According to the test, the photocatalytic activity after 4 h of irradiation for composite coatings based on titanium oxides on the hot-rolled carbon steel and fine-grained concrete is 98 % and 97 %, respectively. Under UV irradiation (Fig. 7), a total discoloration is achieved on the samples with composite coatings based on titanium oxides. Discoloration of rhodamine B on the surface of sample «composite coatings based on titanium oxides /fine-grained concrete» occurred after 1 h.

Table 3

- Discoloration of RhB on the surface of composite coatings based on titanium oxides (exposure time 4 h).

Ti-TiO ₂ coating /Substrate	Coordinate		Discoloration R ₄ ,%
	a ₀	a ₄	
hot-rolled carbon steel	18.32	0.3	98
fine-grained concrete	16.96	0.56	97

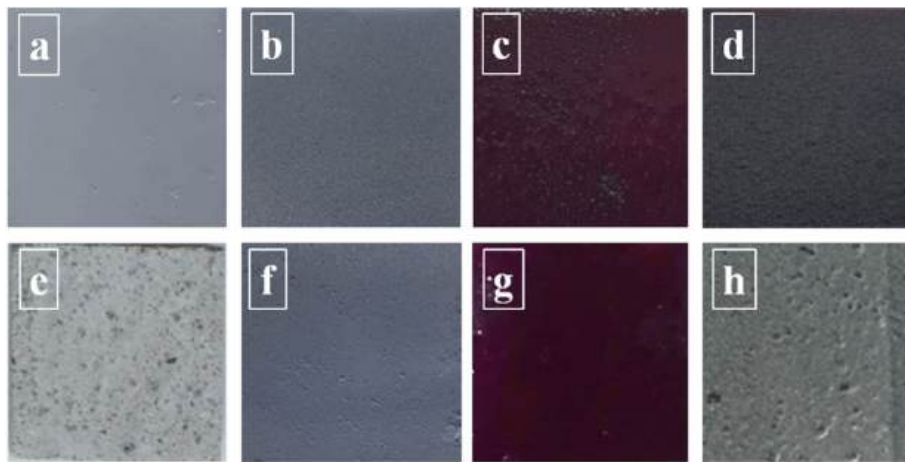


Fig. 7. Rhodamine B discoloration under UV irradiation on the surface of the samples: steel (a); coating /steel (b); coating /steel /RhB (c); coating /steel /RhB /UV (d); concrete (e); coating /concrete (f); coating /concrete /RhB (g); coating /concrete /RhB /UV (g).

3.4. Photocatalytic wettability

The photocatalytic response of composite coatings based on titanium oxides has been measured by means of wettability response under a UV light incidence in the area where the oleic acid drop was collocated. If the coating presents a super-hydrophilic response to the UV light beam, a photocatalytic reaction can be considered [92]. The change in wettability of samples under UV light irradiance can be appreciated in Fig. 8 and Table 4.

Before the start of the experiment, the initial contact angle (without organic pollutant) (column 1, Table 4) was determined for the samples as a reference one, which should be reached by the end of the study after the surface was completely cleaned of the pollutant. Then, oleic acid was applied to the surface of the samples and the initial contact angle was determined (column 2, Table 4), after which the samples were placed under an ultraviolet irradiator.

The first measurement was taken after 1 h, and then the time intervals between measurements were 3 h. The values and time to reach the final contact angle (CA) are shown in Table 4 (columns 3 and 5). The control samples were kept without illumination from the radiation source and external illumination (column 4, Table 4).

When the CA is $>90^\circ$, it is considered that the surface repels the spreading of the water drop, thus exhibiting a low wettability, i.e., hydrophobicity. If the CA is higher than 150° , the phenomenon is known as superhydrophobicity [93]. On the other hand, if the CA is $<90^\circ$, the surface is considered to be highly wettable and exhibiting hydrophilicity properties [15].

Table 4

- Photocatalytic wettability test results for the composite coatings based on titanium oxides (the average value of the contact angle (wetting angle) (ISO 27448:2009).

substrate	Contact angle, deg.				Time to reach the final contact angle, h
	Initial	End	Control		
	without organic dye	with organic dye	after irradiating with UV light	without UV light	
steel	72.96	114.39	65.96	96.11	16
concrete	41.22	89.85	66.92	107.16	31

All samples showed the ability to self-clean the previously contaminated surface under the influence of ultraviolet radiation. This result is consistent with those reported in Refs. [15,39,94–96].

Photocatalytic decomposition of oleic acid, confirmed by a decrease in the value of the contact angle to the final one, occurred for composite coatings based on titanium oxides on the hot-rolled carbon steel substrate in 16 h. For the composite coatings based on titanium oxides on the fine-grained concrete, a long period (31 h) of increase in the surface contact angle from the initial value was observed.

However, the photocatalytic degradation of oleic acid occurred in both cases much faster than expected by the test conditions. The composite coatings based on titanium oxides on the hot-rolled carbon steel and fine-grained concrete are showed high photocatalytic activity. The decomposition time of oleic acid is due to the different roughness of the

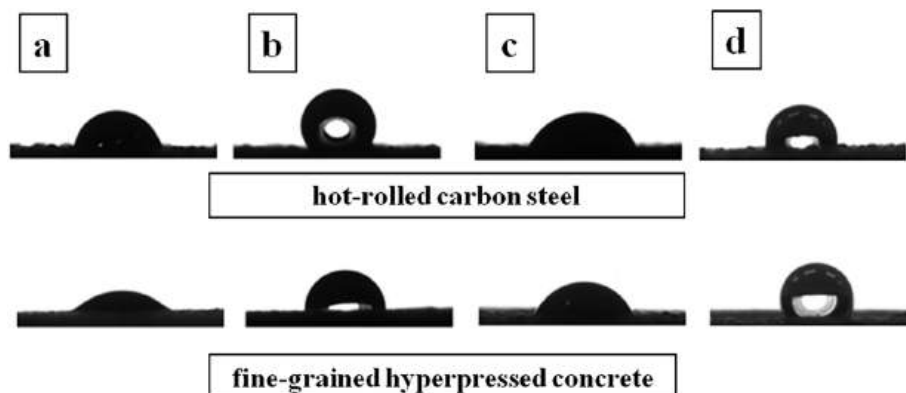


Fig. 8. Photocatalytic wettability test results for the composite coatings based on titanium oxides: the initial contact angle without organic dye (a); the initial contact angle with organic dye (b); the final contact angle with organic dye after irradiating with UV light (c); control contact angle without UV (d).

samples. The surface of the coating on concrete has a large roughness, which is due to the porosity of the substrate.

4. Conclusions

The composite coatings based on titanium oxides were successfully deposited on the hot-rolled carbon steel and fine-grained concrete substrates using a robotic complex for detonation spraying of coatings equipped with a multi-chamber detonation accelerator. The structural, morphological, chemical composition and photocatalytic activity of these samples were investigated by different methods such as XRD, SEM, and XPS. In order to evaluate the efficacy of the coatings, the resultant photocatalytic activity has been monitored by three different tests.

The most salient observations can be summarized as follows:

- The resulting composite coatings based on titanium oxides have a dense lamellar structure as observed in common thermally sprayed coatings, 100–150 μm and 150–200 μm thick on the hot-rolled carbon steel and fine-grained concrete substrates, respectively. Pores are very fine and uniformly scattered.
- XRD analysis revealed that the coatings are mainly composed of rutile (36.0–44.5 %) and anatase (22.3–24.0 %).
- The composite coatings based on titanium oxides showed photocatalytic activity for the degradation of various organic substances under UV irradiation.
- The photocatalytic activity was 95 % according to ISO 10678:2010 (E) (change in methylene blue concentration), 98 % according to UNI 11259 (discoloration of the organic dye Rhodamine B).
- The photocatalytic activity was 16 h on the hot-rolled carbon steel and 31 h on fine-grained concrete according to ISO 27448:2009 (photocatalytic decomposition of oleic acid on the surface of the test sample).
- The values of the kinetic constant of the obtained coatings were much higher than those of the commercial sol-gel coating, and corresponded to the values indicated for thermally sprayed coatings.

The obtained results show that coatings obtained by detonation sputtering can be a good alternative to existing photocatalytic coatings based on TiO_2 . These coatings have high functional properties (strength, corrosion and photocatalytic) and can be used in various industries, in particular, to prevent fouling of ships and offshore structures made of metals or concrete by microorganisms and algae.

Declaration of competing interest

The authors declare that they have no known competing financial interests or personal relationships that could have appeared to influence the work reported in this paper.

Acknowledgments

The study was carried within the framework of the implementation of the state task of the Ministry of Science and Higher Education of the Russian Federation No FZWN-2023-0006. Investigations were carried out using the equipment of the Center of High Technologies of the Belgorod State Technological University after V.G. Shukhov, an unique scientific installation No 3552744, and the equipment of the Joint Research Center “Technologies and Materials” of the Belgorod National Research University.

References

- [1] D.J. Howell, S.M. Evans, Antifouling materials, in: J.K. Cochran, H.J. Bokuniewicz, P.L. Yager (Eds.), *Encyclopedia of Ocean Sciences*, Elsevier, 2009, pp. 236–242, <https://doi.org/10.1016/B978-0-12-813081-0.00764-3>.
- [2] M. Strokhal, Z. Bai, W. Franssen, N. Hofstra, A.A. Koelmans, F. Ludwig, L. Ma, P. van Puijenbroek, J.E. Spanier, L.C. Vermeulen, M.T.H. van Vliet, J. van Wijnen,

- C. Kroeze, Urbanization: an increasing source of multiple pollutants to rivers in the 21st century, *Npj. Urban Sustain.* 1 (1) (2021) 24, <https://doi.org/10.1038/s42949-021-00026-w>.
- [3] A. Tsatsakis, D. Petrakis, T.K. Nikolouzakis, A.O. Docea, D. Calina, M. Vinceti, M. Goumenou, R.N. Kostoff, C. Mamoulakis, M. Aschner, A.F. Hernández, COVID-19, an opportunity to reevaluate the correlation between long-term effects of anthropogenic pollutants on viral epidemic/pandemic events and prevalence, *Food Chem. Toxicol.* 141 (2020), 111418, <https://doi.org/10.1016/j.fct.2020.111418>.
- [4] A.K. Thakur, R. Sathyamurthy, R. Velraj, I. Lynch, R. Saidur, A.K. Pandey, S. W. Sharshir, A.E. Kabeel, J.Y. Hwang, P. Ganesh Kumar, Secondary transmission of SARS-CoV-2 through wastewater: concerns and tactics for treatment to effectively control the pandemic, *J. Environ. Manag.* 290 (2021), 112668, <https://doi.org/10.1016/j.jenvman.2021.112668>.
- [5] Y. Liu, J. Huang, X. Feng, H. Li, Thermal-sprayed photocatalytic coatings for biocidal applications: a review, *J. Therm. Spray Technol.* 30 (1–2) (2021) 1–24, <https://doi.org/10.1007/s11666-020-01118-2>.
- [6] M. Faraldos, R. Kropp, M.A. Anderson, K. Sobolev, Photocatalytic hydrophobic concrete coatings to combat air pollution, *Catal. Today* 259 (1) (2016) 228–236, <https://doi.org/10.1016/j.cattod.2015.07.025>.
- [7] K. Atacan, N. Güy, M. Özacar, Recent advances in photocatalytic coatings for antimicrobial surfaces, *Cur. Opin. Chem. Eng.* 36 (2022), 100777, <https://doi.org/10.1016/j.coche.2021.100777>.
- [8] R. Katal, S. Masudy-Panah, M. Tanhaei, M.H.D.A. Farahani, H. Jiangyong, A review on the synthesis of the various types of anatase TiO_2 facets and their applications for photocatalysis, *J. Chem. Eng.* 384 (2020), 123384, <https://doi.org/10.1016/j.cej.2019.123384>.
- [9] A. Yamakata, J.J.M. Vequizo, Curious behaviors of photogenerated electrons and holes at the defects on anatase, rutile, and brookite TiO_2 powders: a review, *J. Photochem. Photobiol., C* 40 (2019) 234–243, <https://doi.org/10.1016/j.jphotochemrev.2018.12.001>.
- [10] Y.-L. Men, P. Liu, X. Peng, Y.-X. Pan, Efficient photocatalysis triggered by thin carbon layers coating on photocatalysts: recent progress and future perspectives, *Sci. China Chem.* 63 (10) (2020) 1416–1427, <https://doi.org/10.1007/s11426-020-9767-9>.
- [11] I.C. Roata, C. Croitoru, A. Pascu, E.M. Stanciu, Photocatalytic coatings via thermal spraying: a mini-review, *AIMS Mater. Sci.* 6 (3) (2019) 335–353, <https://doi.org/10.3934/matersci.2019.3.335>.
- [12] B. Pant, M. Park, S.J. Park, Recent advances in TiO_2 films prepared by sol-gel methods for photocatalytic degradation of organic pollutants and antibacterial activities, *Coatings* 9 (10) (2019) 613, <https://doi.org/10.3390/coatings9100613>.
- [13] G. Kenanakis, D. Vernardou, A. Dalamagkas, N. Katsarakis, Photocatalytic and electrooxidation properties of TiO_2 thin films deposited by sol-gel, *Catal. Today* (2015) 146–152, <https://doi.org/10.1016/j.cattod.2014.05.007>, 240(PA).
- [14] P. Dullian, W. Nacht, J. Jaglarz, P. Zięba, J. Kanak, W. Żukowski, Photocatalytic methylene blue degradation on multilayer transparent TiO_2 coatings, *Opt. Mater.* 90 (2019) 264–272, <https://doi.org/10.1016/j.optmat.2019.02.041>.
- [15] S. Obregón, V. Rodríguez-González, Photocatalytic TiO_2 thin films and coatings prepared by sol-gel processing: a brief review, *J. Sol. Gel Sci. Technol.* 102 (1) (2022) 125–141, <https://doi.org/10.1007/s10971-021-05628-5>.
- [16] L. Francioso, D.S. Presicce, P. Siciliano, A. Ficarella, Combustion conditions discrimination properties of Pt-doped TiO_2 thin film oxygen sensor, *Sensor. Actuator. B Chem.* 123 (2007) 516–521, <https://doi.org/10.1016/j.snb.2006.09.037>.
- [17] Y. Wang, Z. Huang, R.S. Gurney, D. Liu, Superhydrophobic and photocatalytic PDMS/TiO_2 coatings with environmental stability and multifunctionality, *Colloids Surf. A Physicochem. Eng. Asp.* 561 (2019) 101–108, <https://doi.org/10.1016/j.colsurfa.2018.10.054>.
- [18] F. Xu, T. Wang, H.Y. Chen, J. Bohling, A.M. Maurice, L. Wu, S. Zhou, Preparation of photocatalytic TiO_2 -based self-cleaning coatings for painted surface without interlayer, *Prog. Org. Coating* 113 (2017) 15–24, <https://doi.org/10.1016/j.porgcoat.2017.08.005>.
- [19] L. Mardare, L. Benea, Development of anticorrosive polymer nanocomposite coating for corrosion protection in marine environment, *IOP Conf. Ser. Mater. Sci. Eng.* 209 (1) (2017), 012056, <https://doi.org/10.1088/1757-899X/209/1/012056>.
- [20] M.T. Islam, A. Dominguez, R.S. Turley, H. Kim, K.A. Sultana, M.A.I. Shuvo, B. Alvarado-Tenorio, M.O. Montes, Y. Lin, J. Gardea-Torresdey, J.C. Noveron, Development of photocatalytic paint based on TiO_2 and photopolymer resin for the degradation of organic pollutants in water, *Sci. Total Environ.* 704 (2020), 135406, <https://doi.org/10.1016/j.scitotenv.2019.135406>.
- [21] M. Taheri, M. Jahanfar, K. Ogino, Self-cleaning traffic marking paint, *Surface. Interfac.* 9 (2017) 13–20, <https://doi.org/10.1016/j.surfin.2017.07.004>.
- [22] L. Weihao, C. Shengnan, W. Jianxun, J. Shaohui, S. Chenlu, L. Yong, H. Gaorong, Study on structural, optical and hydrophilic properties of FTO/TiO_2 tandem thin film prepared by aerosol-assisted chemical vapor deposition method, *Surf. Coat. Technol.* 358 (2019) 715–720, <https://doi.org/10.1016/j.surfcoat.2018.11.098>.
- [23] K. Yang, S. Zhong, H. Yue, S. Tang, K. Ma, C. Liu, K. Qiao, B. Liang, Application of pulsed chemical vapor deposition on the SiO_2 -coated TiO_2 production within a rotary reactor at room temperature, *Chin. J. Chem. Eng.* 45 (2022) 22–31, <https://doi.org/10.1016/j.cjche.2021.05.012>.
- [24] B. Astinchap, K.G. Laelabadi, Effects of substrate temperature and precursor amount on optical properties and microstructure of CVD deposited amorphous TiO_2 thin films, *J. Phys. Chem. Solid.* 129 (2019) 217–226, <https://doi.org/10.1016/j.jpcs.2019.01.012>.
- [25] A.K. Singh, V. Chaudhary, A.K. Singh, S.R.P. Sinha, Effect of TiO_2 nanoparticles on electrical properties of chemical vapor deposition grown single layer graphene,

- Synth. Met. 256 (2019), 116155, <https://doi.org/10.1016/j.synthmet.2019.116155>.
- [26] B. Astinchap, H. Ghanbaripour, R. Amuzgar, Multifractal study of TiO₂ thin films deposited by MO-CVD method: the role of precursor amount and substrate temperature, *Optik* 222 (2020), 165384, <https://doi.org/10.1016/j.ijleo.2020.165384>.
- [27] J. Sung, M. Shin, P.R. Deshmukh, H.S. Hyun, Y. Sohn, W.G. Shin, Preparation of ultrathin TiO₂ coating on boron particles by thermal chemical vapor deposition and their oxidation-resistance performance, *J. Alloys Compd.* 767 (2018) 924–931, <https://doi.org/10.1016/j.jallcom.2018.07.152>.
- [28] C. Lee, H. Choi, C. Lee, H. Kim, Photocatalytic properties of nano-structured TiO₂ plasma sprayed coating, *Surf. Coat. Technol.* 173 (2–3) (2003) 192–200, [https://doi.org/10.1016/S0257-8972\(03\)00509-7](https://doi.org/10.1016/S0257-8972(03)00509-7).
- [29] N. Sharifi, A. Dolatabadi, M. Pugh, C. Moreau, Anti-icing performance and durability of suspension plasma sprayed TiO₂ coatings, *Cold Reg. Sci. Technol.* 159 (2019) 1–12, <https://doi.org/10.1016/j.coldregions.2018.11.018>.
- [30] W. Zhang, J. Gu, C. Zhang, Y. Xie, X. Zheng, Preparation of titania coating by induction suspension plasma spraying for biomedical application, *Surf. Coat. Technol.* 358 (2019) 511–520, <https://doi.org/10.1016/j.surfcoat.2018.11.047>.
- [31] W. Seremak, A. Baszczuk, M. Jasiorski, A. Gibas, M. Winnicki, Photocatalytic activity enhancement of low-pressure cold-sprayed TiO₂ coatings induced by long-term water vapor exposure, *J. Therm. Spray Technol.* 30 (7) (2021) 1827–1836, <https://doi.org/10.1007/s11666-021-01244-5>.
- [32] M. Winnicki, L. Latka, M. Jasiorski, A. Baszczuk, Mechanical properties of TiO₂ coatings deposited by low pressure cold spraying, *Surf. Coat. Technol.* 405 (2021), 126516, <https://doi.org/10.1016/j.surfcoat.2020.126516>.
- [33] K. Schmidt, S. Buhl, N. Davoudi, C. Godard, R. Merz, I. Raid, E. Kerscher, M. Kopnarski, C. Müller-Renno, S. Ripperger, J. Seewig, C. Ziegler, S. Antonyuk, Ti surface modification by cold spraying with TiO₂ microparticles, *Surf. Coat. Technol.* 309 (2017) 749–758, <https://doi.org/10.1016/j.surfcoat.2016.10.091>.
- [34] M. Winnicki, A. Gibas, A. Baszczuk, M. Jasiorski, Low pressure cold spraying of TiO₂ on acrylonitrile butadiene styrene (ABS), *Surf. Coat. Technol.* 406 (2021), 126717, <https://doi.org/10.1016/j.surfcoat.2020.126717>.
- [35] A. Kozlovskiy, I. Shlimas, K. Dukenbayev, M. Zdorovets, Structure and corrosion properties of thin TiO₂ films obtained by magnetron sputtering, *Vacuum* 164 (2019) 224–232, <https://doi.org/10.1016/j.vacuum.2019.03.026>.
- [36] J. Singh, S.A. Khan, J. Shah, R.K. Kotnala, S. Mohapatra, Nanostructured TiO₂ thin films prepared by RF magnetron sputtering for photocatalytic applications, *Appl. Surf. Sci.* 422 (2017) 953–961, <https://doi.org/10.1016/j.apsusc.2017.06.068>.
- [37] A. Vahl, S. Veziroglu, B. Henkel, T. Strunskus, O. Polonskiy, O.C. Aktas, F. Faupel, Pathways to tailor photocatalytic performance of TiO₂ thin films deposited by reactive magnetron sputtering, *Materials* 12 (7) (2019) 2840, <https://doi.org/10.3390/ma12172840>.
- [38] Y.H. Wang, K.H. Rahman, C.C. Wu, K.C. Chen, A review on the pathways of the improved structural characteristics and photocatalytic performance of titanium dioxide (TiO₂) thin films fabricated by the magnetron-sputtering technique, *Catalyst* 10 (6) (2020) 598, <https://doi.org/10.3390/catal10060598>.
- [39] A.L. Costa, S. Orтели, M. Blosi, S. Albonetti, A. Vaccari, M. Dondi, TiO₂ based photocatalytic coatings: from nanostructure to functional properties, *Chem. Eng. J.* 22 (2013) 880–886, <https://doi.org/10.1016/j.cej.2013.04.037>.
- [40] D.M. Mattox, *Handbook of physical vapor deposition (PVD) processing*, Pierson, H. O. *Handbook of Chemical Vapor Deposition-Principles, Technology and Application*; William Andrew Publishing: New York, NY, USA, 1999, William Andrew, Burlington, VT, USA, 2010.
- [41] Z. Yi, J. Liu, W. Wei, J. Wang, S.-W. Lee, Photocatalytic performance and microstructure of thermal-sprayed nanostructured TiO₂ coatings, *Ceram. Int.* 34 (2) (2008) 351–357, <https://doi.org/10.1016/j.ceramint.2006.10.023>.
- [42] N. Berger-Keller, G. Bertrand, C. Filatre, C. Meunier, C. Coddet, Microstructure of plasma-sprayed titania coatings deposited from spray-dried powder, *Surf. Coat. Technol.* 168 (2–3) (2003) 281–290, [https://doi.org/10.1016/S0257-8972\(03\)00223-8](https://doi.org/10.1016/S0257-8972(03)00223-8).
- [43] G. Bolelli, V. Cannillo, R. Gadow, A. Killinger, L. Lusvarghi, J. Rauch, Properties of high velocity suspension flame sprayed (HVSFS) TiO₂ coatings, *Surf. Coat. Technol.* 203 (12) (2009) 1722–1732, <https://doi.org/10.1016/j.surfcoat.2009.01.006>.
- [44] E. Bannier, G. Darut, E. Sánchez, A. Denoirjean, M.C. Bordes, M.D. Salvador, E. Rayón, H. Ageorges, Microstructure and photocatalytic activity of suspension plasma sprayed TiO₂ coatings on steel and glass substrates, *Surf. Coat. Technol.* 206 (2–3) (2011) 378–386, <https://doi.org/10.1016/j.surfcoat.2011.07.039>.
- [45] M. Bai, R. Khammas, L. Guan, J.W. Murray, T. Hussain, Suspension high velocity oxy-fuel spraying of a rutile TiO₂ feedstock: microstructure, phase evolution and photocatalytic behaviour, *Ceram. Int.* 43 (17) (2017) 15288–15295, <https://doi.org/10.1016/j.ceramint.2017.08.06>.
- [46] G.-J. Yang, C.-J. Li, F. Han, A. Ohmori, Microstructure and photocatalytic performance of high velocity oxy-fuel sprayed TiO₂ coatings, *Thin Solid Films* 466 (1–2) (2004) 81–85, <https://doi.org/10.1016/j.tsf.2004.02.015>.
- [47] M. Bozorgtabar, M. Salehi, M. Rahimpour, M. Jafarpour, Influence of high velocity oxy-fuel parameters on properties of nanostructured TiO₂ coatings, *Bull. Mater. Sci.* 33 (6) (2010) 671–675, <https://doi.org/10.1007/s12034-011-0146-9>.
- [48] F.-L. Toma, L.-M. Berger, C.C. Stahr, T. Naumann, S. Langner, Functional properties of suspension-sprayed Al₂O₃ and TiO₂ coatings: an overview, *J. Therm. Spray Technol.* 19 (2010) 262–274, <https://doi.org/10.1007/s11666-009-9417-z>.
- [49] D.V. Dudina, S.B. Zlobin, N.V. Bulina, A.L. Bychkov, V.N. Korolyuk, V. Yu Ulianitsky, O.I. Lomovsky, Detonation spraying of TiO₂-2.5vol.% Ag powders in a reducing atmosphere, *J. Eur. Ceram. Soc.* 32 (4) (2012) 815–821, <https://doi.org/10.1016/j.jeurceramsoc.2011.10.022>.
- [50] D.V. Dudina, S.B. Zlobin, V. Yu, N. Ulianitsky, V. Bulina, A.L. Bychkov, O. I. Lomovsky, Detonation spraying of TiO₂-Ag powders under a controllable atmosphere, Paper presented at: ITSC 2011, in: Proceedings of the International Thermal Spray Conference and Exposition, ASM International, Hamburg, Germany, 2011, pp. 504–508, <https://doi.org/10.31399/asm.cp.itsc2011p0504>, September 27–29.
- [51] A. Kengesbekov, Z. Sagdoldina, K. Torebek, D. Baizhan, Y. Kambarov, M. Yermolenko, S. Abdulina, M. Maulet, Synthesis and formation mechanism of metal oxide compounds, *Coatings* 12 (2022) 1511, <https://doi.org/10.3390/coatings12101511>.
- [52] S. Panin, I. Vlasov, D. Dudina, V. Ulianitsky, R. Stankevich, I. Batraev, F. Berto, Mechanical characterization of composite coatings formed by reactive detonation spraying of titanium, *Metals* 7 (2017) 355, <https://doi.org/10.3390/met7090355>.
- [53] M. Kovaleva, Yu Tyurin, O. Kolisnichenko, M. Prozorova, M. Arsenenko, Properties of detonation nanostructured titanium-based coatings, *J. Therm. Spray Technol.* 22 (4) (2013) 518–524, <https://doi.org/10.1007/s11666-013-9909-8>.
- [54] Y.A. Nikolaev, A.A. Vasiliev, V.Y. Ulianitsky, Gas detonation and its application in engineering and technologies, submitted for publication, *Combust. Explos. Shock Waves* 39 (2003) 382–410, <https://doi.org/10.1023/A:1024726619703>.
- [55] A. Sova, D. Pervushin, I. Smurov, Development of multimaterial coatings by cold spray and gas detonation spraying, *Surf. Coat. Technol.* 205 (4) (2010) 1108–1114, <https://doi.org/10.1016/j.surfcoat.2010.07.092>.
- [56] M.Yu Arsenenko, M.S. Prozorova, M.G. Kovaleva, V.Yu Novikov, M.N. Yaprntsev, V.V. Sirota, I.A. Pavlenko, YuN. Tyurin, Deposition and characterization of the titanium-based coating by a multi-chamber detonation sprayer, *MATEC Web Conf* (30) (2015), 01008, <https://doi.org/10.1051/mateconf/20153001008>.
- [57] M. Kovaleva, Yu Tyurin, N. Vasilik, O. Kolisnichenko, M. Prozorova, M. Arsenenko, V. Sirota, I. Pavlenko, Structure and microhardness of titanium-based coatings formed by multi-chamber detonation sprayer, *Physiother. Res. Int.* 2015 (2015), 532825, <https://doi.org/10.1155/2015/532825>.
- [58] D.V. Dudina, G.A. Pribytkov, M.G. Krinitcyn, M.A. Korchagin, N.V. Bulina, B. B. Bokhonov, I.S. Batraev, D.K. Rybin, V.Yu Ulianitsky, Detonation spraying behavior of Ti-Cu powders and the role of reactive processes in the coating formation, *Ceram. Int.* 42 (1) (2016) 690–696, <https://doi.org/10.1016/j.ceramint.2015.08.166>.
- [59] V.Y. Ulianitsky, D.V. Dudina, A.A. Shtertser, I. Smurov, Computer-controlled detonation spraying: flexible control of the coating chemistry and microstructure, *Metals* 9 (2019) 1244, <https://doi.org/10.3390/met9121244>.
- [60] A.A. Shtertser, I.S. Batraev, V.Yu Ulianitsky, I.D. Kuchumova, N.V. Bulina, A. V. Ukhina, B.B. Bokhonov, D.V. Dudina, P.V. Trinh, D.D. Phuong, Detonation spraying of Ti-Cu mixtures in different atmospheres: carbon, nitrogen and oxygen uptake by the powders, *Surface. Interfac.* 21 (2020), 100676, <https://doi.org/10.1016/j.surfint.2020.100676>.
- [61] M. Kovaleva, I. Goncharov, V. Novikov, I. Pavlenko, M. Yaprntsev, O. Vagina, V. Sirota, Yu Tyurin, O. Kolisnichenko, V. Krasil'nikov, Oxidation behavior and microstructural evolution of ZrB₂-35MoSi₂-10Al composite coating, *Coatings* 11 (9) (2021) 1231, <https://doi.org/10.3390/coatings11121531>.
- [62] V. Sirota, V. Pavlenko, N. Cherkashina, M. Kovaleva, Y. Tyurin, O. Kolisnichenko, Preparation of aluminum oxide coating on carbon/carbon composites using a new detonation sprayer, *Int. J. Appl. Ceram. 2* (2021) 483–489, <https://doi.org/10.1111/ijac.13671>.
- [63] V. Sirota, S. Zaitsev, D. Prokhorenkov, M. Limarenko, A. Skiba, M. Kovaleva, NiB-CrC coatings prepared by magnetron sputtering using composite ceramic NiCr-BC target produced by detonation spray coating, *Nanomaterials* 12 (20) (2022) 3584, <https://doi.org/10.3390/nano12203584>.
- [64] N. Vasilik, Yu Tyurin, O. Kolisnichenko, Method for gas-dynamic detonating speedup of powders and device for its implementation, *RU Patent* (2012) 11, 2506341.
- [65] Yu Tyurin, O. Kolisnichenko, J. Jia, N. Vasilik, M. Kovaleva, M. Prozorova, M. Arsenenko, V. Sirota, Performance and economic characteristics of multi-chamber detonation sprayer used in thermal spray technology, in: Paper Presented at: ITSC 2016. Proceedings of the International Thermal Spray Conference and Exposition, ASM International, Shanghai, China, 2016, pp. 630–634, <https://doi.org/10.31399/asm.cp.itsc2016p0630>, 2016 May 10–12.
- [66] M. Kovaleva, M. Prozorova, M. Arsenenko, Y. Tyurin, O. Kolisnichenko, M. Yaprntsev, V. Novikov, O. Vagina, V. Sirota, Zircon-based ceramic coatings formed by a new multi-chamber gas-dynamic accelerator, *Coatings* 7 (2017) 142, <https://doi.org/10.3390/coatings7090142>.
- [67] G.J. Moskal, The porosity assessment of thermal barrier coatings obtained by APS method, *J. Achiev. Mater. Manuf.* 20 (1–2) (2007) 483–486.
- [68] G. Ji, Y. Zou, C. Chen, H. Yao, X. Bai, C. Yang, H. Wang, F. Wang, Mechanical properties of warm sprayed HATI bio-ceramic composite coatings, *Ceram. Int.* 46 (17) (2020) 27021–27030, <https://doi.org/10.1016/j.ceramint.2020.07.179>.
- [69] K.A. Khor, Y. Wang, P. Cheang, Thermal spraying of functionally graded coatings for biomedical applications, *Surf. Eng.* 14 (2) (1998) 159–164, <https://doi.org/10.1179/sur.1998.14.2.159>.
- [70] I. Khan, K. Saeed, I. Zekker, B. Zhang, A.H. Hendi, A. Ahmad, S. Ahmad, N. Zada, H. Ahmad, L.A. Shah, T. Shah, I. Khan, Review on methylene blue: its properties, uses, toxicity and photodegradation, *Water* 14 (2022) 242, <https://doi.org/10.3390/w14020242>.
- [71] ISO/DIS 10678: Fine Ceramics (Advanced Ceramics, Advanced Technical Ceramics): Determination of Photocatalytic Activity of Surfaces in an Aqueous Medium by Degradation of Methylene Blue, (standard under development).
- [72] UNI 11259: Determination of the Photocatalytic Activity of Hydraulic Binders Radamina Test Method.

- [73] B. Ruot, A. Plassais, F. Olive, L. Guillot, L. Bonafous, TiO₂-containing cement pastes and mortars: measurements of the photocatalytic efficiency using a rhodamine B based colourimetric test, *Sol. Energy* 83 (10) (2009) 1794–1801, <https://doi.org/10.1016/j.solener.2009.05.017>.
- [74] L. Bonafous, L. Cassar, P. Cassat, P. Colombet, L. Guillot, et al., *Photocatalytic Granular Mixture for Mortar and Concrete and its Use*, 2009. US 7,556,683 B2. ISO 27448, *Fine Ceramics (Advanced Ceramics, Advanced Technical Ceramics) - Test Method for Self-Cleaning Performance of Semiconducting Photocatalytic Materials - Measurement of Water Contact Angle*, NEQ, 2009.
- [75] A. Skopp, N. Kelling, M. Woydt, L.-M. Berger, Thermally sprayed titanium suboxide coatings for piston ring/cylinder liners under mixed lubrication and dry-running conditions, *Wear* 262 (2007) 1061–1070, <https://doi.org/10.1016/j.wear.2006.11.012>.
- [76] P. Citbor, K. Neufuss, P. Chraska, Microstructure and abrasion resistance of plasma sprayed titania coatings, *J. Therm. Spray Technol.* 15 (2006) 689–694, <https://doi.org/10.1361/105996306X146749>.
- [77] D.V. Dudina, I.S. Batraev, YuV. Ulianitsky, M.A. Korzhagin, Possibilities of the computer-controlled detonation spraying method: a chemistry viewpoint, *Ceram. Int.* 40 (2014) 3253–3260, <https://doi.org/10.1016/j.ceramint.2013.09.111>.
- [78] V.Yu Ulianitsky, D.V. Dudina, I.S. Batraev, A.I. Kovalenko, N.V. Bulina, B. B. Bokhonov, Detonation spraying of titanium and formation of coatings with spraying atmosphere-dependent phase composition, *Surf. Coat. Technol.* 261 (2015) 174–180, <https://doi.org/10.1016/j.surfcoat.2014.11.038>.
- [79] W. Wong, E. Irissou, A.N. Ryabinin, J.-G. Legoux, S. Yue, Influence of helium and nitrogen gases on the properties of cold gas dynamic sprayed pure titanium coatings, *J. Therm. Spray Technol.* 20 (1–2) (2011) 213–226, <https://doi.org/10.1007/s11666-010-9568-y>.
- [80] H. Okamoto, O-Ti (Oxygen-Titanium), *J. Phase Equilibria Diffus.* 32 (5) (2011) 473–474, <https://doi.org/10.1007/s11669-011-9935-5>.
- [81] J. Colmenares-Angulo, S. Zhao, C. Young, A. Orlov, The effects of thermal spray technique and post-deposition treatment on the photocatalytic activity of TiO₂ coatings, *Surf. Coat. Technol.* 204 (4) (2009) 423–427, <https://doi.org/10.1016/j.surfcoat.2009.07.046>.
- [82] E. Bemporad, G. Bolelli, V. Cannillo, D. De Felicis, R. Gadow, A. Killinger, L. Lusvarghi, J. Rauch, M. Sebastiani, Structural characterisation of high velocity suspension flame sprayed (HVSFS) TiO₂ coatings, *Surf. Coat. Technol.* 204 (23) (2010) 3902–3910, <https://doi.org/10.1016/j.surfcoat.2010.05.011>.
- [83] F.-L. Toma, L.-M. Berger, D. Jacquet, D. Wicky, I. Villaluenga, Y.R. de Miguel, J. S. Lindeløv, Comparative study on the photocatalytic behaviour of titanium oxide thermal sprayed coatings from powders and suspensions, *Surf. Coat. Technol.* 203 (15) (2009) 2150–2156.
- [84] S. Kozerski, F.-L. Toma, L. Pawlowski, B. Leupolt, L. Latka, L.-M. Berger, Suspension plasma sprayed TiO₂ coatings using different injectors and their photocatalytic properties, *Surf. Coat. Technol.* 205 (4) (2010) 980–986, <https://doi.org/10.1016/j.surfcoat.2010.04.068>.
- [85] V. Binas, D. Papadaki, Th Maggos, A. Katsanaki, G. Kiriakidis, Study of innovative photocatalytic cement based coatings: the effect of supporting materials, *Construct. Build. Mater.* 168 (2018) 923–930, <https://doi.org/10.1016/j.conbuildmat.2018.02.106>.
- [86] P. Peerakiatkhajohn, T. Butburee, J.-H. Sul, S. Thaweesak, J.-H. Yun, Efficient and rapid photocatalytic degradation of methyl orange dye using Al/ZnO nanoparticles, *Nanomaterials* 11 (2021) 1059, <https://doi.org/10.3390/nano11041059>.
- [87] A. Farzanex, M. Javidani, M. Esrafil, O. Mermer, Optical and photocatalytic characteristic of Al and Cu doped TiO₂: experimental assessment and DFT calculations, *J. Phys. Chem. Solid.* 161 (2021), 110404, <https://doi.org/10.1016/j.jpcs.2021.110404>.
- [88] D. Komaraiah, E. Radha, J. Sivakumar, M.V. Ramana, R.R. Sayanna, Photoluminescence and photocatalytic activity of spin coated Ag⁺ Doped anatase TiO₂ thin films, *Opt. Mater.* 108 (2020), 110401, <https://doi.org/10.1016/j.optmat.2020.110401>.
- [89] E. Assayehegn, A. Solaiappan, Y. Chebude, E. Alemayehu, Fabrication of tunable anatase/rutile heterojunction N/TiO₂ nanophotocatalyst for enhanced visible light degradation activity, *Appl. Surf. Sci.* 515 (2020), 145966, <https://doi.org/10.1016/j.apsusc.2020.145966>.
- [90] U. Chinonso, O. Ibukun, H.K. Jeong, Air plasma treated TiO₂/MWCNT composite for enhanced photocatalytic activity, *Chem. Phys. Lett.* 757 (2020), 137850, <https://doi.org/10.1016/j.cplett.2020.137850>.
- [91] R. De Sun, A. Nakajima, A. Fujishima, T. Watanabe, K. Hashimoto, Photoinduced surface wettability conversion of ZnO and TiO₂ thin films, *J. Phys. Chem. B* 105 (2001) 1984–1990, <https://doi.org/10.1021/jp002525j>.
- [92] F. Geyer, M. D'Acunzi, A. Sharifi-Aghili, A. Saal, N. Gao, A. Kaltbeitzel, T.F. Sloot, R. Berger, H.J. Butt, D. Vollmer, When and how self-cleaning of superhydrophobic surfaces works, *Sci. Adv.* 6 (2020), eaaw9727, <https://doi.org/10.1126/sciadv.aaw9727>.
- [93] X. Sandua, P.J. Rivero, A. Conde, J. Esparza, R. Rodríguez, A Comparative study in the design of TiO₂ assisted photocatalytic coatings monitored by controlling hydrophilic behavior and rhodamine B degradation, *Materials* 16 (7) (2023) 2589, <https://doi.org/10.3390/ma16072589>.
- [94] T. Adachi, S.S. Latthe, S.W. Gosavi, N. Roy, N. Suzuki, H. Ikari, K. Kato, K. Katsumata, K. Nakata, M. Furudate, T. Inoue, T. Kondo, M. Yuasa, A. Fujishima, C. Terashima, Photocatalytic, superhydrophilic, self-cleaning TiO₂ coating on cheap, light-weight, flexible polycarbonate substrates, *Appl. Surf. Sci.* 458 (2018) 917–923, <https://doi.org/10.1016/j.apsusc.2018.07.172>.
- [95] L. Cassar, A. Beeldens, N. Pimpinelli, G.L. Guerrini, *Photocatalysis of cementitious materials*, in: *Proceedings of the International Rilem Symposium on Photocatalysis*, 2007. Florence, Italy, 8–9 October.